

## A CoMFA Study of Quinazoline-based Anticancer Agents

Anand Balupuri<sup>1†</sup>, Pavithra K. Balasubramanian<sup>1</sup>, and Seung Joo Cho<sup>1,2†</sup>

### Abstract

Cancer has emerged as one of the leading cause of deaths worldwide. A three-dimensional quantitative structure-activity relationship (3D-QSAR) analysis was performed on a series of quinazoline-based anticancer agents. Purpose of the study is to understand the structural basis for their inhibitory activity. Comparative molecular field analysis (CoMFA) technique was employed to develop 3D-QSAR model. Ligand-based alignment scheme was used to generate a reliable CoMFA model. The model produced statistically significant results with a cross-validated correlation coefficient ( $q^2$ ) of 0.589 and a non-cross-validated correlation coefficient ( $r^2$ ) of 0.928. Model was further validated by bootstrapping and progressive scrambling analysis. This study could assist in the design of novel and more potent anticancer agents.

**Key words:** Cancer, Quinazoline-based Anticancer agents, 3D-QSAR, CoMFA

### 1. Introduction

Cancer is among the leading cause of death worldwide<sup>[1]</sup>. The number of deaths due to cancer is expected to reach approximately 13.1 million by 2030. Many bioactive compounds have been reported to possess anticancer activity<sup>[2]</sup>. However, their use as anticancer agents is limited because of the side effects or the limited scope. Hence, the identification of novel, potent drugs with a broad spectrum of activity and fewer side effects is required for the improvement of cancer treatment. Antimitotic agents which interact with microtubules are widely used in the cancer chemotherapy<sup>[3-7]</sup>. Microtubules or tubulin protein polymers are a major component of the cytoskeleton of eukaryotic cells. Tubulin proteins can polymerize as well as depolymerize, and microtubules can undergo rapid cycles of assembly and disassembly. Antimitotic agents interact with tubulin either at the colchicine-, vinblastine- or paclitaxel-binding site<sup>[8]</sup>. These agents either inhibit or promote microtubule polymerization and accordingly affect their function.

Tremendous efforts have been made to develop anticancer agents and a number of antimitotic compounds have been synthesized as promising drug candidates<sup>[9]</sup>. Recently, quinazoline-based anticancer agents were reported<sup>[10]</sup>. However, a three-dimensional quantitative structure-activity relationship (3D-QSAR) analysis on these inhibitors has not been performed to establish exactly how their chemical structures relate to the inhibitory activities. Our research group is involved in molecular modeling studies<sup>[11-15]</sup>. Here, we have performed comparative molecular field analysis (CoMFA) to identify the key structural elements that are required in the rational design of novel drug candidates.

### 2. Experimental Section

#### 2.1. Data Set

A data set of 45 quinazoline-based anticancer agents was collected<sup>[10]</sup>. Reported activity values ( $IC_{50}$ ) of inhibitors were converted into  $pIC_{50}$  values for 3D-QSAR analysis. Converted  $pIC_{50}$  values were used as the dependent variables for developing CoMFA model. The energy minimized structure of the most active compound (**28**) was used as template to construct other compounds of the data set. All 3D structures were sketched using SYBYL-X2.0<sup>[16]</sup>. Gasteiger-Hückel partial atomic charges were applied to the structures. Energy minimization was performed using Tripos force field. The minimized structures were aligned to the

<sup>1</sup>Department of Biomedical Science, College of Medicine, Chosun University, Gwangju 501-759, Korea

<sup>2</sup>Department of Cellular · Molecular Medicine, College of Medicine, Chosun University, Gwangju 501-759, Korea

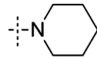
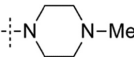
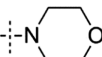
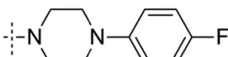
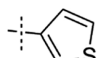
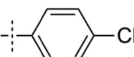
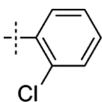
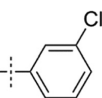
†Corresponding author : [anandbalupuri.niper@gmail.com](mailto:anandbalupuri.niper@gmail.com),  
[chosj@chosun.ac.kr](mailto:chosj@chosun.ac.kr)

(Received: June 30, 2015, Revised: September 17, 2015,  
Accepted: September 25, 2015)

**Table 1.** Chemical structures and biological activities of quinazoline-based anticancer agents

Compound	R <sub>1</sub>	R <sub>2</sub>	R <sub>3</sub>	IC <sub>50</sub> (iM)	pIC <sub>50</sub>
1	4-OMe	Me	H	0.27	6.5686
2	4-F	Me	H	>25	4.6021
3	4-Cl	Me	H	>25	4.6021
4	4-CF <sub>3</sub>	Me	H	>25	4.6021
5	H	Me	H	>25	4.6021
6	4-OEt	Me	H	0.30	6.5229
7*	4-O <sup>t</sup> Bu	Me	H	>25	4.6021
8	4-OCF <sub>3</sub>	Me	H	>25	4.6021
9	3-OMe	Me	H	>25	4.6021
10	3,4-OCH <sub>2</sub> O-	Me	H	20	4.6990
11	3,4-OMe	Me	H	21	4.6778
12	3,4,5-OMe	Me	H	>25	4.6021
13	3-OBn	Me	H	>25	4.6021
14	3-OH	Me	H	>25	4.6021
15	4-NHMe	Me	H	4.1	5.3872
16	4-NMe <sub>2</sub>	Me	H	1.3	5.8861
17*	4-SMe	Me	H	0.34	6.4685
18	4OMe		H	20	4.6990
19	4-OEt		H	>25	4.6021
20	4-OMe	Et	H	1.8	5.7447
21	4-OMe	Bn	H	9.8	5.0088
22	4-OMe	CF <sub>3</sub>	H	1.1	5.9586
23	4-OMe	H	H	>25	4.6021
24*				2.0	5.6990
25	4-OMe	Me	Me	0.053	7.2757
26	4-OMe	Me	Ph	0.1	7.0000
27	4-OMe	Me	CCl <sub>3</sub>	0.038	7.4202
28	4-OMe	Me	Cl	0.027	7.5686
29*				>25	4.6021
30	4-OMe	Me	OMe	0.058	7.2366
31	4-OMe	Me	OEt	0.34	6.4685

**Table 1.** Chemical structures and biological activities of quinazoline-based anticancer agents

Compound	R <sub>1</sub>	R <sub>2</sub>	R <sub>3</sub>	IC <sub>50</sub> (iM)	pIC <sub>50</sub>
32	4-OMe	Me	OPr	1.2	5.9208
33	4-OMe	Me	Oallyl	0.41	6.3872
34	4-OMe	Me	OPh	3.3	5.4815
35	4-OMe	Me	SMe	0.067	7.1739
36	4-OMe	Me	NMe <sub>2</sub>	20.21	6.6778
37	4-OMe	Me	NHPh	2.7	5.5686
38	4-OMe	Me		2.7	5.5686
39	4-OMe	Me		19	4.7212
40	4-OMe	Me		0.17	6.7696
41	4-OMe	Me		1.9	5.7212
42	4-OMe	Me		0.035	7.4559
43	4-OMe	Me		0.40	6.3979
44	4-OMe	Me		0.78	6.1079
45	4-OMe	Me		2.1	5.6778

\*Compounds are considered as outliers.

template molecule using common substructure-based alignment method. Chemical structures and biological activities of the compounds are given in Table 1.

## 2.2. CoMFA

CoMFA calculations were performed using SYBYL-X2.0. CoMFA technique is based on the assumption that variations in the activity of compounds are related to the changes in the steric and electrostatic fields<sup>[17]</sup>. CoMFA steric (Lennard-Jones potential) and electrostatic (Coulomb potential) interaction fields were calculated using default settings. A 3D cubic lattice with a grid spacing of 2.0 Å was created and fields were generated using a sp<sup>3</sup> carbon probe atom carrying +1 charge

and van der Waals radius of 1.50 Å. An energy cut-off of 30 kcal mol<sup>-1</sup> was used for the calculation of interaction fields.

Relationship between structural parameters and biological activities was derived using Partial least squares (PLS) regression algorithm<sup>[18]</sup>. CoMFA descriptors were used as independent variables while pIC<sub>50</sub> values were used as dependent variables in the PLS analysis. The leave-one-out (LOO) cross-validation was carried out to obtain cross-validated correlation coefficient (q<sup>2</sup>), optimal number of components (NOC) and standard error of prediction (SEP). The non-cross-validated analysis was performed to obtain non-cross-validated correlation coefficient (r<sup>2</sup>), standard error of estimate (SEE)

and F-test value (F). Developed CoMFA model was validated using bootstrapping analysis<sup>[19]</sup> and progressive scrambling. Bootstrapping of 100 runs and a total of 100 independent scramblings with a maximum of 10 bins and a minimum of 2 bins were carried out.

### 3. Results and Discussion

#### 3.1. CoMFA Model

CoMFA model was developed using a series of quinazoline-based anticancer agents. Model was generated from the whole data set using ligand-based alignment scheme. All data set compounds were aligned over the template (compound **28**) using common substructure alignment method. The aligned compounds are displayed in Fig. 1. Data set was not divided into training and test sets during model generation. Four compounds (**7**, **17**, **24** and **29**) were removed from data set as outliers during model development. Compounds **7** and **17** displayed high residual values whereas compounds **24** and **29** were structurally different from rest of the data set compounds.

A reliable CoMFA model in terms of several statistical parameters was obtained. The detailed statistical values for the model are given in Table 2. Model displayed a  $q^2$  value of 0.589 with 5 components. The non-cross-validated analysis produced  $r^2$ , SEE and F values of 0.928, 0.291 and 90.859, respectively. The steric and electrostatic contributions were 60.6% and 39.4%, respectively. Actual and predicted activity values along with the residual values for compounds are listed in

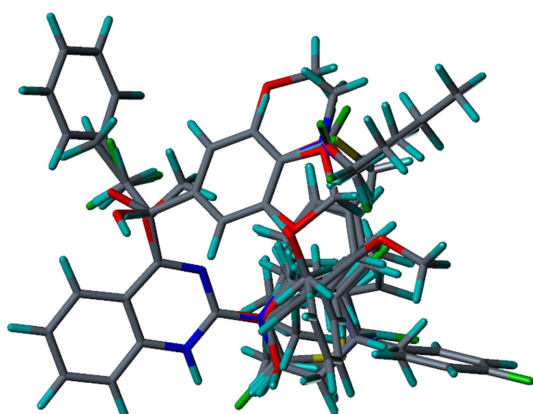


**Fig. 1.** Common substructure-based alignment of data set compounds using compound **28** as a template.

**Table 2.** Statistical parameters of the CoMFA model

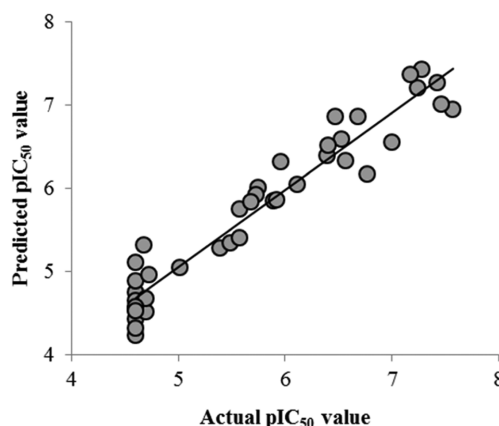
Parameters	CoMFA
$q^2$	0.589
NOC	5
SEP	0.698
$r^2$	0.928
SEE	0.291
F	90.859
BS- $r^2$	0.951
BS-sd	0.014
$Q^2$	0.461
Steric contribution	60.6
Electrostatic contribution	39.4

Note:  $q^2$  is cross-validated correlation coefficient, NOC is number of components, SEP is standard error of prediction,  $r^2$  is non-cross-validated correlation coefficient, SEE is standard error of estimation; F is F-test value, BS- $r^2$  is bootstrapping  $r^2$  mean, BS-SD is bootstrapping standard deviation,  $Q^2$  is corrected  $q^2$  dependency.

Table 3. The scatter plot for actual versus predicted  $pIC_{50}$  values is shown in Fig. 2. Predicted activities are in agreement with the experimental values suggesting that a reliable CoMFA model was developed.

#### 3.2. CoMFA Contour Maps

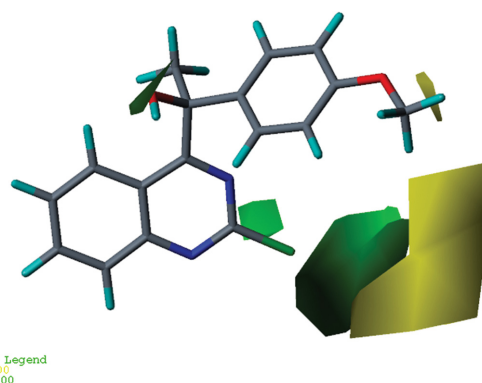
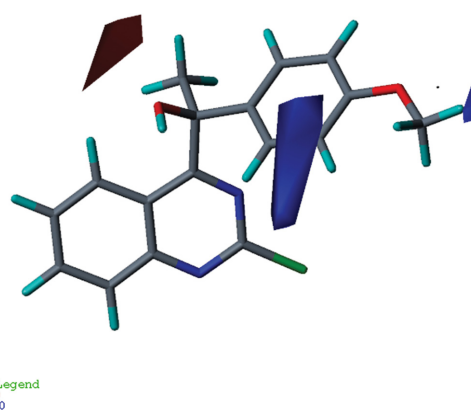
The CoMFA results were graphically interpreted by the field contribution maps. The contour maps of different fields are displayed with template (compound **28**). Maps describe default 80% and 20% level contributions for favorable and unfavorable regions, respec-



**Fig. 2.** Scatter plot of the actual versus predicted activities based on the CoMFA model.

**Table 3.** Actual and predicted activity values with residuals of the data set compounds

Compound	Actual pIC <sub>50</sub>	CoMFA	
		Predicted pIC <sub>50</sub>	Residual
1	6.5686	6.3400	0.2291
2	4.6021	4.7460	-0.1440
3	4.6021	4.5450	0.0572
4	4.6021	4.4310	0.1706
5	4.6021	4.5550	0.0473
6	6.5229	6.5930	-0.0705
8	4.6021	5.1110	-0.5091
9	4.6021	4.2370	0.3653
10	4.6990	4.5180	0.1814
11	4.6778	5.3240	-0.6460
12	4.6021	4.6570	-0.0545
13	4.6021	4.8830	-0.2811
14	4.6021	4.3240	0.2776
15	5.3872	5.2890	0.0984
16	5.8861	5.8550	0.0312
18	4.6990	4.6720	0.0266
19	4.6021	4.5730	0.0287
20	5.7447	6.0130	-0.2685
21	5.0088	5.0490	-0.0398
22	5.9586	6.3200	-0.3617
23	4.6021	4.5240	0.0779
25	7.2757	7.4310	-0.1548
26	7.0000	6.5520	0.4480
27	7.4202	7.2760	0.1443
28	7.5686	6.9580	0.6106
30	7.2366	7.2170	0.0193
31	6.4685	6.8630	-0.3944
32	5.9208	5.8690	0.0519
33	6.3872	6.4010	-0.0135
34	5.4815	5.3470	0.1347
35	7.1739	7.3800	-0.2063
36	6.6778	6.8680	-0.1903
37	5.5686	5.4070	0.1615
38	5.5686	5.7580	-0.1898
39	4.7212	4.9580	-0.2370
40	6.7696	6.1710	0.5983
41	5.7212	5.9310	-0.2101
42	7.4559	7.0150	0.4409
43	6.3979	6.5250	-0.1269
44	6.1079	6.0470	0.0605
45	5.6778	5.8410	-0.1631

**Fig. 3.** CoMFA steric contour map with template (compound **28**) as a reference. Green contours indicate sterically favored regions while yellow contours indicate sterically unfavorable regions.**Fig. 4.** CoMFA electrostatic contour map with template (compound **28**) as a reference. Blue contours represent favorable regions for electropositive substituents whereas red represent favorable regions for electronegative substituents.

tively. Maps indicate spatial requirement of steric and electrostatic fields for improving the inhibitory activity of the compounds.

Steric contour map is displayed in Fig. 3. Green contours indicate favorable regions whereas yellow contours indicate unfavorable regions for bulky group substitution. A green contours observed near R<sub>3</sub> substitution suggested that bulky groups in this region are favorable for increasing the activity. This could be the possible reason for better inhibitory activities of compounds **25**, **27**, **28** and **30** as compared to compound **1**. Yellow contours observed around R<sub>1</sub> substitution sug-

gested that small groups are favored in this region and bulky substituents could decrease the activity. This might be the possible reason for the lower activities of compounds **2**, **3** and **5** as compared to compounds **6**, **16** and **17**.

Electrostatic contour map is displayed in Fig. 4. Blue contours indicate regions where electropositive substitutions are favored while red contours indicate favorable regions for electronegative substitutions to enhance the activity. Blue contours observed near R<sub>1</sub> substitution suggested that electropositive groups at that position could increase the activity. This could be the possible reason for higher activities of compounds **15**, **16** and **17** than compounds **2** and **3**. The red contour observed near R<sub>2</sub> substitution suggested that electronegative groups at that position could improve the activity. This might be the reason for higher activity of compound **22** than compounds **20** and **23**.

#### 4. Conclusions

In the present study, a CoMFA model was developed for a series of quinazoline-based anticancer agents. The model provided some insights into the crucial structural factors affecting the bioactivity of these anticancer agents. Ligand-based alignment scheme and Gasteiger-Hückel partial charges produced a reliable CoMFA model. The model showed statistically acceptable results in terms of  $q^2$  and  $r^2$  values. Validation results of bootstrapping and progressive sampling also indicated that the developed model is robust. Contour map analysis highlighted regions for chemical modification to improve the inhibitory activity of the compounds. Smaller groups with electropositive properties at R<sub>1</sub> substitution whereas electronegative groups at R<sub>2</sub> substitution and bulky groups at R<sub>3</sub> substitution are desirable to improve the inhibitory potency. These results may provide some useful and rational suggestions for the design of novel and more potent anticancer agents.

#### Acknowledgements

This research was supported by Basic Science Research Program through the National Research Foundation of Korea (NRF) funded by the Ministry of Education, Science and Technology (NRF-2012R1A1A4A01001465).

#### References

- [1] WHO, Cancer, <http://www.who.int/cancer/en/>, 2015.
- [2] V. T. Jr. DeVita and E. Chu, "A history of cancer chemotherapy", *Cancer Res.*, Vol. 68, pp. 8643-8653, 2008.
- [3] S. K. Tahir, E. K. Han, B. Credo, H. S. Jae, J. A. Pietenpol, C. D. Scatena, J. R. Wu-Wong, D. Frost, H. Sham, S. H. Rosenberg, and S. C. Ng, "A-204197, a new tubulin-binding agent with antimetabolic activity in tumor cell lines resistant to known microtubule inhibitors." *Cancer Res.*, Vol. 61, pp. 5480-5485, 2001.
- [4] H. Prinz, Y. Ishii, T. Hirano, T. Stoiber, J. A. Camacho Gomez, P. Schmidt, H. Dössmann, A. M. Burger, J. H. Prehn, E. G. Günther, E. Unger, and K. Umezawa, "Novel benzylidene-9(10H)-anthracenones as highly active antimicrotubule agents. Synthesis, antiproliferative activity, and inhibition of tubulin polymerization", *J. Med. Chem.*, Vol. 46, pp. 3382-3394, 2003.
- [5] R. Romagnoli, P. G. Baraldi, V. Remusat, M. D. Carrion, C. L. Cara, D. Preti, F. Fruttarolo, M. G. Pavani, M. A. Tabrizi, M. Tolomeo, S. Grimaudo, J. Balzarini, M. A. Jordan, and E. Hamel, "Synthesis and biological evaluation of 2-(3',4',5'-trimethoxybenzoyl)-3-amino 5-aryl thiophenes as a new class of tubulin inhibitors", *J. Med. Chem.*, Vol. 49, pp. 6425-6428, 2006.
- [6] A. Davis, J. D. Jiang, K. M. Middleton, Y. Wang, I. Weisz, Y. H. Ling, and J. G. Bekesi, "Novel suicide ligands of tubulin arrest cancer cells in S-phase" *Neoplasia*, Vol. 1, pp. 498-507, 1999.
- [7] M. M. Joullié, S. Berritt, and E. Hamel, "Structure-activity relationships of ustiloxin analogues", *Tetrahedron Lett.*, Vol. 52, pp. 2136-2139, 2011.
- [8] S. Honore, E. Pasquier, and D. Braguer, "Understanding microtubule dynamics for improved cancer therapy", *Cell Mol. Life Sci.*, Vol. 62, pp. 3039-3056, 2005..
- [9] K. M. R. Bhat and V. Setaluri, "Microtubule-associated proteins as targets in cancer chemotherapy", *Clin. Cancer Res.*, Vol. 13, pp. 2849-2854, 2007..
- [10] K. Kuroiwa, H. Ishii, K. Matsuno, A. Asai, and Y. Suzuki, "Synthesis and structure-activity relationship study of 1-phenyl-1-(quinazolin-4-yl)ethanols as anticancer agents", *ACS Med. Chem. Lett.*, Vol. 6, pp. 287-291, 2015.
- [11] A. Balupuri and S. J. Cho, "Exploration of the binding mode of indole derivatives as potent HIV-1 inhibitors using molecular docking simulations", *J.*

- Chosun Natural Sci., Vol. 6, pp. 138-142, 2013.
- [12] A. Balupuri, P. K. Balasubramanian, and S. J. Cho, "A CoMFA study of glycogen synthase kinase 3 inhibitors", *J. Chosun Natural Sci.*, Vol. 8, pp. 40-47, 2015.
- [13] P. K. Balasubramanian, A. Balupuri, and S. J. Cho, "A CoMFA study of phenoxy pyridine-based JNK3 inhibitors using various partial charge schemes", *J. Chosun Natural Sci.*, Vol. 7, pp. 45-49, 2014.
- [14] P. K. Balasubramanian, A. Balupuri, and S. J. Cho, "Ligand-based CoMFA study on pyridylpyrazolopyridine derivatives as PKC $\theta$  kinase inhibitors", *J. Chosun Natural Sci.*, Vol. 7, pp. 253-259, 2014.
- [15] P. K. Balasubramanian and S. J. Cho, "HQ SAR analysis on novel series of 1-(4-phenylpiperazin-1-yl)-2-(1H-Pyrazol-1-yl) ethanone derivatives targeting CCR1", *J. Chosun Natural Sci.*, Vol. 6, pp. 163-169, 2013.
- [16] SYBYLx2.1, Tripos International, South Hanley Road, St. Louis, Missouri, 63144, USA, 1999.
- [17] R. D. Cramer, D. E. Patterson, and J. D. Bunce, "Comparative molecular field analysis (CoMFA). 1. Effect of shape on binding of steroids to carrier proteins", *J. Am. Chem. Soc.*, Vol. 110, pp. 5959-5967, 1988.
- [18] S. Wold, A. Ruhe, H. Wold, and I. W. Dunn, "The collinearity problem in linear regression. The partial least squares (PLS) approach to generalized inverses", *SIAM J. Sci. Comput.*, Vol. 5, pp. 735-743, 1984.
- [19] R. D. Cramer, J. D. Bunce, D. E. Patterson, and I. E. Frank, "Crossvalidation, bootstrapping, and partial least squares compared with multiple regression in conventional QSAR studies", *Quant. Struct. Act. Relat.*, Vol. 7, pp. 18-25, 1988.